Low sensitivity of a heavily-calcified coccolithophore under increasing CO_2: the case study of *Helicosphaera carteri*

Stefania Bianco[†1,2], Manuela Bordiga[†3], Gerald Langer[*4], Patrizia Ziveri[4, 5], Federica Cerino[3], Andrea S. Di Giulio[2], Claudia Lupi[2]

[1]University School for Advanced Studies IUSS of Pavia, Pavia, 27100, Italy
[2]Department of Earth and Environmental Sciences, University of Pavia, Pavia, 27100, Italy
[3]National Institute of Oceanography and Applied Geophysics - OGS, Trieste, 34151, Italy
[4]Institute of Environmental Science and Technology, Universitat Autònoma de Barcelona (ICTA-UAB), Barcelona, 08193, Spain
[5]Catalan Institution for Research and Advanced Studies (ICREA), Barcelona, 08010, Spain

†These authors contributed equally to this work

Correspondence to: Gerald Langer (Gerald.Langer@uab.cat)

Abstract. Studies on CO_2 effects on coccolithophores, unicellular calcifying phytoplankton, show species-specific responses, although only less than 5% of the ~280 living species have been tested so far. *Helicosphaera carteri* significantly contributes to carbon fluxes and $CaCO_3$ storage due to its size and high calcite production. Despite its importance, few studies have examined *H. carteri* under experimental conditions, and only one has addressed the effects of rising CO_2/decreasing pH. Being *H. carter*i a large-sized, obligated calcifier species, an important aspect to understand is how changes in seawater carbonate chemistry may affect its morphology. It has already been suggested for other coccolithophores species, that the presence of malformed coccoliths may represent a disadvantage for these organisms. Moreover, an alteration in coccolith morphology may affect their contribution to $CaCO_3$ sedimentation and ballasting. As for *H. carteri*, it has also been suggested that due to its high PIC:POC ratio, the species could show a ~~high sensitivity~~high sensitivity to CO_2 rise. In this study, we investigate for the first time whether high pCO_2/low pH does affect the morphology of *H. carteri* coccoliths, by culturing this species under pre-industrial CO_2 levels (~295 µatm) and ~600 µatm, i.e., the SSP 2-4.5 scenario for 2100 (IPCC, 2021). We also analyzed cellular PIC and POC quotas using morphometric data, roundness, and protoplast and coccosphere size to observe the pCO_2 influence on the calcification and photosynthesis ratio.

Our results indicate that *H. carteri* morphology is not significantly affected by increasing CO_2, in contrast to other heavily calcified species. *Helicosphaera carteri* protoplast and coccosphere shapes did not vary with changes in CO_2, as did its particulate inorganic carbon (PIC) and particulate organic carbon (POC) quotas, as well as the PIC:POC ratio, indicating unaltered physiological state.

~~Our results indicate that *H. carteri* morphology is only slightly affected by increasing CO_2, in contrast to other heavily calcified species. *Helicosphaera carteri* protoplast and coccosphere shapes did not vary with changes in CO_2, indicating unaltered general health.~~ The low PIC:POC ratio found in this work for *H. carteri* compared to ratios previously measured in

the same strain under different experimental conditions, and compared to other highly-calcified species, could explain the observed low sensitivity of *H. carteri* to CO_2. Moreover, the observation of a stable ratio between calcification and photosynthesis in *H. carteri* under increasing CO_2 might suggest a constant contribution to the rain ratio under climate change. However, further studies comparing experimental and field data from past ocean acidification events will be required to confirm the conclusions drawn here.

1 Introduction

Since the industrial revolution, human activities have led to a rapid increase in atmospheric CO_2 concentration. A large amount of this emitted CO_2 (~30%) is absorbed by the oceans (Canadell et al., 2007; Sabine et al., 2004), causing a significant imbalance in the ocean chemistry, which is moving more and more towards lower pH values (IPCC, 2021).

To date, several studies have focused on the effects of seawater carbonate chemistry on calcifying organisms, including coccolithophores (e.g., D'Amario et al., 2020; Dong et al., 2023; Gattuso et al., 1998; Gazeau et al., 2024; Jokiel et al., 2008; Keul et al., 2013; Langdon et al., 2000; Riebesell et al., 2000; Ries et al., 2011), and different and sometimes contrasting evidence have been collected for this group (e.g., Iglesias-Rodriguez et al., 2008; Kroeker et al., 2013; Langer et al., 2006; Meyer & Riebesell, 2015; Raven & Crawfurd, 2012; Riebesell et al., 2000). Up to now, these studies have also demonstrated that to predict the responses of this group of calcifying microalgae, the consideration of different species, and even strains (Langer et al., 2009) is required. Indeed, while at the beginning, most of the efforts have been focused on common and easy-to-grow species, such as *Emiliania huxleyi* and *Gephyrocapsa oceanica*, in the last two decades, many studies have also focused on other species, like *Calcidiscus leptoporus, Calcidiscus quadriperforatus*, *Coccolithus pelagicus* subsp. *braarudii* and *Scyphosphaera apsteinii* (e.g., Diner et al., 2015; Fiorini et al., 2011; Gafar et al., 2019a, b; Krug et al., 2011; Langer et al., 2006; Langer and Bode, 2011). The latter species are characterized by lower abundances compared to *E. huxleyi*, but nevertheless play an important role in coccolithophore $CaCO_3$ production in modern oceans (Baumann et al., 2004; Daniels et al., 2014, 2016; Gafar et al., 2019b; Menschel et al., 2016; Ziveri et al., 2007).

Another low-abundant but highly contributing to $CaCO_3$ production is *Helicosphaera carteri* that is considered one of the main contributors to carbon (C) export and storage into deep-sea sediments (Ziveri et al., 2007), thanks to its large size and higher rates of organic C fixation and calcite production, compared to smaller species (García-Romero et al., 2017; Menschel et al., 2016; Rigual Hernández et al., 2020; Young & Ziveri, 2000). Indeed, while *E. huxleyi* produces between ~6 and ~20 pg cell^{-1} day^{-1} of calcite, *H. carteri* produces ~~more than~~between ~80 120~~100~~ pg ~~C~~ cell^{-1} day^{-1} of calcite (De Bodt et al., 2010; Langer et al., 2009; Šupraha et al., 2015).

Helicosphaera carteri is generally considered to be a species typical of warm waters (e.g., Baumann et al., 2005; Brand, 1994), with moderately high-nutrient levels (e.g., Andruleit and Rogalla, 2002; Findlay and Giraudeau, 2000, 2002; Ziveri et al., 1995, 2004). However, it has a general wide distribution (as reported in the CASCADE database; de Vries et al., 2024) and it seems to be an opportunistic species, easily adaptable to different environmental conditions (Dimiza et al., 2014 and

references therein). This adaptability of *H. carteri* is confirmed by its long fossil record, spanning back more than 20 Million years (Aubry, 1988; Young 1998).

Despite its relevant role, only a few studies have been conducted on living *H. carteri* under experimental conditions (e.g., Sheward et al., 2017; Šupraha et al., 2015; Šupraha & Henderiks 2020) and only one of them ~~took into account~~considered the effects of CO_2 increase on this species (Le Guevel et al., 2024). To assess the potential effects of CO_2 increasing/pH lowering on coccolithophores, it is fundamental to study not only changes in calcite production, but also in coccolith morphology, as previously suggested by Langer et al. (2011). Indeed, despite the coccosphere's function is still unclear and might differ among species (Monteiro et al., 2016), studies on coccolithogenesis and coccolith structure and morphology have suggested that these calcite plates represent an advantage, and in some cases a necessity, for coccolithophores (e.g., Henriksen et al., 2003; Langer et al., 2021; Walker et al., 2018). Coccoliths morphology represents a key factor in their ecology (Bown et al., 2004; Young, 1994) and the inhibition or alteration of coccolithophores' ability to calcify can be detrimental for most of the species belonging to this group, as demonstrated by Walker et al. (2018) for *C. braarudii*. Previous studies have also shown that increasing CO_2/decreasing pH can strongly affect coccolithogenesis and coccolith morphology, especially when considering species bearing big-sized and heavily-calcified coccoliths, with a possible detrimental influence on the ability of these organisms to face future climate changes (Diner et al., 2015; Kottmeier et al., 2022; Langer et al., 2006; Langer and Bode 2011).

Given the importance of *H. carteri*'s role in the C cycle, we investigate here for the first time whether rising pCO_2 does affect coccolith morphology in this species by analyzing the presence of malformations in *H. carteri* cultures grown under pre-industrial CO_2 levels (~290 µatm) and ~600 µatm i.e., scenario SSP 2-4.5 for 2100 (IPCC, 2021). Additionally, we analyze variations in cellular particulate organic (POC), and inorganic (PIC) carbon using morphometric data (e.g., protoplast size, number of coccoliths per coccosphere, coccolith length) and investigate the variations in protoplast and coccosphere size and roundness (RD).

2 Materials and methods

2.1 Experimental setting and chemical analyses

Monospecific cultures of *Helicosphaera carteri* (strain RCC1323, from Southern Benguela upwelling area of South Atlantic from Roscoff Culture Collection) were grown in natural sterile-filtered seawater collected in the Gulf of Trieste (northern Adriatic Sea, Italy), filtered through 0.22 µm pore size Durapore membrane filters (Millipore) and autoclaved, and enriched with vitamins, nutrients, and trace elements following the B medium recipe (https://cosmi.ogs.it/node/7). Culture experiments were performed at the National Institute of Oceanography and Applied Geophysics (OGS) in Trieste using the dilute batch culture method (Langer et al., 2013) and keeping constant salinity (35 PSU), temperature (19°C), light irradiance (100 µmol m^{-2} s^{-1}), light/dark cycle (12:12 hours) under two different levels of CO_2 (295 and 600 µatm) in 2.5L photobioreactors (Kbiotech) controlled by the BioFlex software. A pitched-blade impeller at 100 rpm rotational speed

ensured the culture agitation. Before starting the experiments at different CO_2 levels, the strain was acclimated for ca. 11 generations to the selected CO_2 concentration. Both experiments were run in triplicate. All the experiments were terminated in the exponential phase at low cell density (ca. 10,000 cell mL^{-1}), i.e., in dilute batch mode, corresponding to 6 or 7 days from the inoculation.

To calculate the pH values corresponding to the two selected carbon dioxide concentrations, Total Alkalinity (TA) was measured before starting the experiments. Then, inserting TA, temperature, salinity, phosphate, and silicate data in the CO2SYS program (Lewis and Wallace, 1998), using the constants of Mehrbach et al. (1973) refitted by Dickson and Millero (1987), we identified a pH of 8.18 for 295 µatm, and 7.81 for 600 µatm. The pH was maintained constant for the entire duration of the experiments by CO_2 injection into the headspace or by adding NaOH (1M) in the culture through an automated peristaltic pump controlled by the BioFlex software. The pH was measured with a sensor (Hamilton PHI 225; sensitivity 57-59 mV; frequency of measurements 10 seconds) inserted within the photobioreactor.

To better characterize the carbonate system and the equilibrium among the parameters involved, Dissolved Inorganic Carbon (DIC) and Total Alkalinity (TA) were measured in two replicas on the final day of the experiment as follows.

For DIC analysis, the culture was filtered through pre-combusted 0.7 µm nominal pore size glass fiber filters (Whatman GF/F), and two samples of 50 mL were collected minimizing gas exchange with the atmosphere, and then poisoned with mercuric chloride ($HgCl_2$) solution in order to prevent biological activity. Samples were stored refrigerated until analyzed. DIC was determined using the Shimadzu TOC-V CSH analyzer (Shimadzu Corporation, Japan). For DIC, samples were injected into the instrument port and directly acidified with phosphoric acid (25%). Phosphoric acidification for DIC and combustion conducted at 680°C, generated CO_2 that was carried to a non-dispersive infrared detector (NDIR). The variation coefficient of the analyses was <2%; and the reproducibility of the method ranged between 1.5 and 3%. Typical OA scenarios do not feature decreasing DIC concentrations. In our experiment the lowest DIC is ca 1400 µM (high CO_2, low pH) and the highest ca 1700 µM (low CO_2, high pH, Table 1). Despite this atypical CO_2-DIC combination for OA scenarios the latter does not undermine the suitability of our experimental setup because DIC is not the parameter of the C-system affecting coccolithophores in typical OA studies (Bach et al., 2011; Hoppe et al., 2011; Langer and Bode, 2011). Only under DIC concentrations below ca. 1000 µM, DIC and/or bicarbonate ion concentration might play a role too (Buitenhuis, 1999). The parameters of the C-system that will have affected *H. carteri* most likely are either pH or CO_2 (Bach et al., 2011; Langer and Bode, 2011); a possible but unlikely candidate is carbonate ion concentration. All three parameters fall within the range of typical OA studies (e.g., Bach et al., 2011; Hoppe et al., 2011; Kottmeier et al., 2022; Johnson et al., 2022; Langer et al., 2009; Langer and Bode, 2011; Milner et al., 2016; Zondervan et al., 2002). Therefore, our experimental setup is suitable for our purpose.

For the TA, 100 mL of culture were filtered through pre-combusted 0.7 µm nominal pore size glass fiber filters (Whatman GF/F), poisoned with 100 µL of saturated mercuric chloride ($HgCl_2$) to halt the biological activity, and stored in acid-washed borosilicate flasks at 4°C. TA was measured by potentiometric titration in an open cell (SOP 3b, Dickson et al., 2007) utilizing a non-linear least squares approach. The titration was conducted with the Mettler Toledo G20 titration unit

interfaced with a computer, using the LabX data-acquisition software. After titration, data were processed and the TA was calculated using a computer program developed at OGS and adapted to work in association with the Mettler Toledo LabX software and similar to that listed in SOP 3 of DOE (Dickson and Goyet, 1994). The HCl titrant solution (0.1 mol kg^{-1}) was prepared in NaCl background, to approximate the ionic strength of the samples, and was calibrated using certified reference seawater (CRM, Batch #107, provided by A.G. Dickson, Scripps Institution of Oceanography, USA). Accuracy and precision of the TA measurements on CRM were determined to be less than ± 2.0 µmol kg^{-1}.

The final carbonate system was calculated from temperature, salinity, TA, pH (NBS), phosphate and silicate, using the CO2SYS program (Lewis and Wallace, 1998), with the same constants mentioned above. The data for the carbonate system are reported in Table 1.

Parameter	Exp. 295	Exp. 600
CO_2 (µatm)	294.6	601.5
SD	17.84	59.74
CO_2 (µmol/kg)	9.78	19.94
SD	0.59	1.98
HCO_3^- (µmol/kg)	1413.49	1213.70
SD	106.02	144.50
CO_3^{2-} (µmol/kg)	141.44	51.72
SD	16.62	13.38
DIC (µmol/kg)	**1677.50**	**1374.72**
SD	**140.87**	**142.03**
TA (mmol/kg^{-1})	**1853.82**	**1452.54**
SD	**166.93**	**146.41**
pH NBS	**8.18**	**7.81**
SD	**0.025**	**0.064**

Formatted: Font: Not Bold

Formatted: Font: Not Bold

Formatted: Font: Not Bold

Formatted: Font: Not Bold

Formatted: Font color: Text 1

Formatted: Font: Bold, Font color: Text 1

Formatted: Font color: Text 1

Formatted: Font: Bold, Font color: Text 1

Formatted: Font color: Text 1

Formatted: Font color: Text 1

Formatted: Font: Bold, Font color: Text 1

Ω calcite	3.38	1.24	
SD	0.40	0.32	

Table 1. Parameters of the carbonate system. In black are the values obtained from the CO2SYS program; in blue are the average values directly measured in duplicates per each replica of both the experiments. The average pH values are derived from the whole data collected in continuum along the experiments (pH standard deviation 0.01).

Formatted: Font: Not Bold

Formatted Table

2.2 Morphological analyses

Helicosphaera carteri coccospheres were collected from triplicate cultures and filtered on cellulose acetate filters (Ø 25 mm pore Ø 0.45 µm) for subsequent analyses at the Scanning Electron Microscope (SEM). Filters were dried at 30°C for 24 hours. The filters were mounted using carbon tapes on SEM stubs, and then sputter-coated with gold-palladium using the Emitech K550X/K250 C cathodic metallizer. Analyses at SEM were conducted with a Zeiss Merlin at the Microscopy and X-ray Diffraction Service of the Universitat Autònoma de Barcelona.

After a preliminary observation of the samples, we subdivided the morphologies of *H. carteri* coccoliths in two main categories: normal and malformed (Fig. 1). At the SEM we observed that the malformations occurring in *H. carteri* coccoliths are often characterized by underdevelopment or abnormal development of the flange (Fig. 1c, d). Sometimes, the malformation is also represented by coccoliths presenting a "wavy" shape (Fig. 1c, d). Per sample at least 100 coccoliths were counted, for a total of ~300 coccoliths per experiment (Table 2).

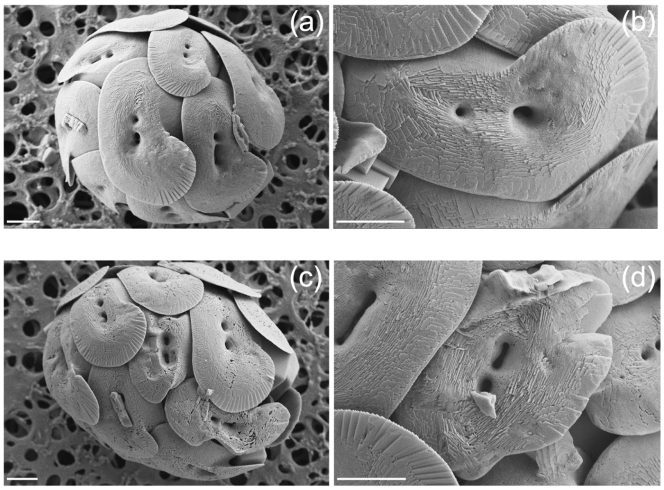

Figure 1. Scanning electron micrographs of *Helicosphaera carteri* coccoliths. (a, b) normal (c, d) malformed. Scale bars are 2 µm.

2.3 Morphometric analyses

2.3.1 Coccosphere measurements and PIC calculation

On the last day of each experiment, 1mL of culture was collected and combined with 4 µL of Formalin for coccosphere morphometric analysis. Coccosphere size (Ø), aspect ratio ($AR_{coccosphere}$) and roundness ($RD_{coccosphere}$) data were obtained by photographing more than 50 coccospheres per each replicate using an inverted microscope Leica CMS-D35578 at 400x magnification and a Leica Camera Ltd CH-9435. The images were processed with ImageJ software (Rueden et al., 2017; Appendix A Fig. A1) using a customized macro (https://github.com/mbordiga/Coccoliths). The estimated standard error of the mean are 0.1219 for Ø, 0.006119 for $AR_{coccosphere}$ and 0.004549 for $RD_{coccosphere}$ at 295 µatm; while at 600µatm are: for 0.1233 Ø, 0.006399 for $AR_{coccosphere}$ and 0.004781 for $RD_{coccosphere}$.

~~Coccosphere size (Ø), aspect ratio ($AR_{coccosphere}$) and roundness ($RD_{coccosphere}$) data were obtained by photographing more than 50 coccospheres per each replicate using an inverted microscope Leica CMS-D35578 and a Leica Camera Ltd CH-9435. The images were processed with ImageJ software (Rueden et al., 2017; Appendix A Fig. A1) using a customized macro (https://github.com/mbordiga/Coccoliths).~~ $AR_{coccosphere}$ and $RD_{coccosphere}$ were strongly correlated (-0.99, p-value <0.0001); therefore, only RD data have been discussed in this work. RD values closer to 1 indicate a more circular shape (for details see Appendix A Table A1).

The cellular particulate inorganic carbon (cellular PIC) of *H. carteri* was estimated from coccosphere geometry data, following Young and Ziveri (2000):

$$\frac{PIC[pg]}{cell} = C_N \times C_L^3 \times K_s \times \rho \times \left(\frac{M_C}{M_{CaCO_3}}\right), \quad (1)$$

Where C_N is the number of coccoliths per coccosphere, C_L^3 is the coccolith length (µm), k_s is the mean species-specific dimensionless shape factor (0.05 for *H. carteri*; Young and Ziveri 2000), ρ is the calcite density (2.7 pg µm^3) and $\frac{M_C}{M_{CaCO_3}}$ is the molar mass ratio of C and $CaCO_3$ (0.12).

The number of coccoliths per cell (C_N) was determined from the samples previously used for counting malformed coccoliths (see Sect. 2.2). At least 50 photographs of coccospheres were captured using the SEM and the number of coccoliths per cell was estimated by visually counting the visible ones and assuming they represent 75% of the total (as demonstrated for *E. huxleyi* in Hoffmann et al., 2015).

The averages data used for the calculation and the number of individuals analyzed are reported in the Appendix (Appendix A Table A1).

For single coccolith measurements, additional culture samples were obtained by treating 25 mL of culture with 25 mL of a Triton (1%) and 20 microL bleach solution to separate them from the cell (see Šupraha & Henderiks, 2020).

Part of the obtained pellet was then added to a solution of distilled water buffer with ammonia (1L distilled water + 30 mL of 25% ammonia solution). A small amount of this suspension was subsequently pipetted onto a round glass coverslip (Ø 13 mm) and dried on a hot plate at 60°C. The coverslip was then mounted on SEM stubs (Ø 25 mm) using a carbon disc. To increase the sample's conductivity, four aluminum bridges connecting the coverslip to the edge of the stubs were added in each sample. The samples were then sputter-coated with platinum and analyzed using the Tescan Mira3XMU SEM of the Department of Earth and environmental Sciences at the University of Pavia (CISRiC-Arvedi Laboratory). Unfortunately, due to an alteration in the preservation state of the material, it was not possible to analyze the third replicate of both experiments. For the remaining samples, at least 100 coccoliths were photographed and measured using ImageJ software (Rueden et al., 2017) for a total of 409 coccoliths (Appendix A Table A1).

Statistical analyses (unpaired t-tests) have been performed for Ø and $RD_{coccosphere}$ using GraphPad Prism (version 9.05 for MacOS; GraphPad Software, Inc., USA).

2.3.2 Protoplast measurements and POC calculation

Helicosphaera carteri cellular POC was estimated from protoplast size, following Menden-Deuer and Lessard (2000):

$$\frac{POC\ [pg]}{cell} = a \times V_{cell}^{b}\ , \qquad (2)$$

Where V_{cell}^{b} is the protoplast volume, and a and b are constants depending on the considered species (in this case: a=0.216 and b=0.939; Menden-Deuer and Lessard, 2000). Protoplast volume in µm was calculated as $V_{cell} = (\pi/6)d^2h$, where d and h represent the short and the long-axes cell diameters in µm (Sun and Liu, 2003).

The V_{cell} was obtained by measuring cells from culture samples collected at the T_{final} of each experiment. 4 mL of culture samples were fixed with acidic Lugol solution (40 µL) which dissolves the coccoliths while preserving the protoplast for subsequent measurements. Protoplast size (Θ) data were obtained by analyzing at least 50 photos (collected at the inverted microscope) per sample, with ImageJ software (Rueden et al., 2017) using a custom-made macro (https://github.com/mbordiga/Coccoliths; Supplementary materials).

With the same macro, data about protoplast aspect ratio ($AR_{protoplastl}$) and roundness ($RD_{protoplast}$), were obtained. As for the coccosphere, due to the high correlation between RD and AR, only data about cellular roundness were reported in this work. The averages of the data used for the calculation and the number of individuals analyzed are provided in the Appendix (Appendix A Table A1).

Changes in Θ and $RD_{protoplast}$ have been compared using an unpaired t-test on GraphPad Prism (version 9.05 for MacOS; GraphPad Software, Inc., USA).

3 Results

3.1 Coccolith morphology

The analyses at the SEM reveal a non-significant change (t-test p value >0.05) in the proportion of malformed coccoliths moving from ~295 to 600 µatm of CO_2. However, while at the lower pCO_2, the species shows almost no malformations (0.66±0.58%) in the second treatment the malformed coccoliths account for an average of 10.65±10.82% (Table 2, Fig. 2). The percentage of malformed coccoliths at 600 µatm is characterized by a high standard deviation (SD), suggesting a relatively high variability among the triplicates. On the contrary, at 295 µatm, SD is quite low in all the considered categories, reflecting a greater degree of consistency between the samples compared to 600 µatm (Table 2).

None of the observed samples shows extremely malformed coccoliths. A rough estimation of the number of collapsed coccospheres per sample indicates a percentage far below 1%. Therefore, a specific count for this category has not been performed, because it is not meaningful. ~~The analyses at the SEM revealed a slight change in the proportion of malformed coccoliths moving from ~295 to 600 µatm of CO_2. Indeed, while at the lower pCO_2, the species shows almost no malformations (0.66%), an increase in the percentage of malformed coccoliths is observed in the second treatment, where the~~

~~normal coccoliths account for an average of 89.35 % (Table 2, Fig. 2). The percentage (10.65%) of malformed coccoliths at 600 µatm is characterized by a high standard deviation (SD), suggesting a relatively high variability among the triplicates. On the contrary, at 295 µatm, SD is quite low in all the considered categories, reflecting a greater degree of consistency between the samples compared to 600 µatm (Table 2). None of the observed samples showed extremely malformed coccoliths. All coccospheres were intact. A rough estimation of the number of collapsed coccospheres per sample indicated a percentage far below 1%. Therefore, a specific count for this category was not performed, because it is not meaningful.~~

The saturation state of seawater with respect to calcite ($\Omega_{calcite}$), was~~is~~ lower at 600 µatm than at pre-industrial CO_2 levels. However, the values ~~are~~ were always >1, indicating that the system ~~is~~ was never undersaturated, indeed no dissolution ~~has been~~was detected (Table 1).

Experiment	CO_2 [µatm]	Normal	Malformed	Total nr. of counted coccoliths
1	295	99.34	0.66	304
SD		2.08	0.58	
2	600	89.35	10.65	316
SD		13.87	10.82	

Table 2. Percentages of counted coccoliths at the two different CO_2 concentrations. Data reported are averages of three replicates. SD = standard deviation.

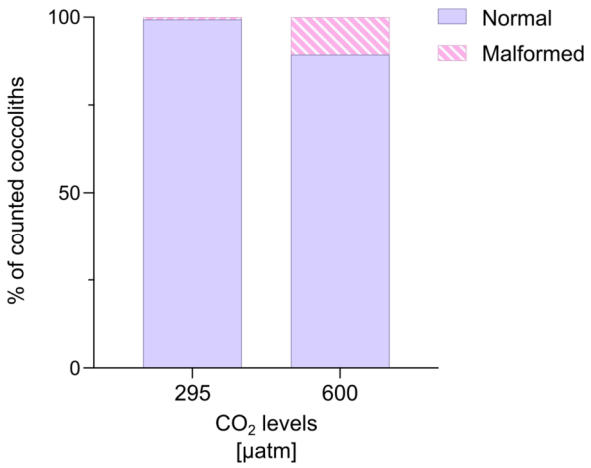

Figure 2. Percentages (%) of normal and malformed coccoliths of *H. carteri*. Values reported represent the averages of the three replicates.

3.2 Coccosphere and protoplast geometry

Cellular POC returns an average of 108.14±5.42 pg cell^{-1} at 295 µatm and 118.51±6.41 pg cell^{-1} at 600 µatm of CO_2. The unpaired t-test indicates that moving from the lowest to the highest CO_2 level, the cellular POC does not change significantly (t-test p value>0.05; Table 3). A non-significant change is also observed in cellular PIC and in the PIC:POC ratio, showing an average value of 150.66±1.59 pg cell^{-1} (t-test p value>0.05; Table 3) and of 1.32±0.07, respectively (t-test p value >0.05; Table 3).~~Cellular POC returns an average of 108.14 pg cell^{+} at 295 µatm and 118.51 pg cell^{+} at 600 µatm of CO_2. The unpaired t-test (performed in GraphPad Prism version 9.05 for MacOS; GraphPad Software, Inc., USA) indicates that the increase from the lowest to the highest CO_2 level is not statistically significant (Table 3). A non-significant change is also observed in cellular PIC, with values varying from 151.86 pg cell^{+} at 295 µatm to 149.47 pg cell^{+} in the second treatment. The PIC:POC ratio does not change significantly (Unpaired t-test p value = 0.2083) as well, decreasing from 1.37 at 295 µatm to 1.27 at 600 µatm of CO_2 (Table 3).~~

Helicosphaera carteri protoplast (0.90±0.06 µm/µm) and coccosphere (0.89±0.05 µm/µm) roundness does not show any significant variation with increasing CO_2 (t-test p value>0.05), indicating the maintenance of a constant shape at different CO_2 levels (Fig. 3a, b; Appendix A Table A1). ~~*Helicosphaera carteri* protoplast and coccosphere roundness does not show~~

~~any significant variation with increasing CO_2. While the first remained unchanged at the value of 0.9 ± 0.06, the second decreased from 0.89 ± 0.05 to 0.88 ± 0.06 indicating the maintenance of a constant shape at different CO_2 levels (Fig. 3 a, b).~~ No changes have been detected for protoplast (11.63 ±0.26 µm; t-test p value>0.05; Fig. 3c; Appendix A Table A1) and coccosphere size (18.05 ±0.18 µm; t-test p value>0.05; Fig. 3d; Appendix A Table A1). ~~A non-significant change in protoplast and coccosphere size with increasing CO_2 can also be observed, with the protoplast size increasing from 11.45 to 11.81 µm and the coccosphere size decreasing from 18.18 to 17.92 µm (Fig. 3 c, d; Appendix A Table A1).~~ The range of protoplast size does not change very much, from 295 to 600 µatm; while for the coccosphere size, a slightly higher range is recorded at the higher CO_2 level (Fig. 3 c, d; Appendix A Table A1).

CO_2 [µatm]		**295**	**600**	**p value**
PIC [pg cell^{-1}]	Mean	151.86	149.47	0.7755
	SD	4.23	9.49	
POC [pg cell^{-1}]	Mean	108.14	118.51	0.1000
	SD	~~22.54~~5.42	~~23.71~~6.41	
PIC:POC		1.37	1.27	0.09595
	SD	0.072	0.013	

Table 3. Data of *H. carteri* cellular PIC and POC obtained from geometry data. Values reported are averages of the replicates. SD = standard deviation.

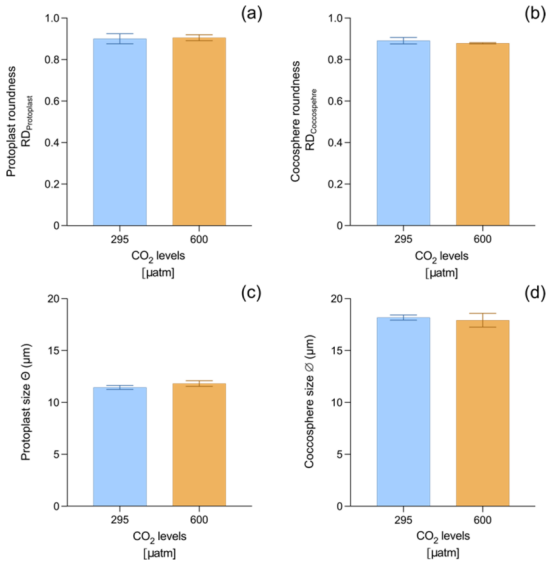

Figure 3. Data of *H. carteri* roundness and size, measured on the protoplast (a, c) and coccosphere (b, d). Reported values are averages of three replicates. Error bars show standard deviation.

4 Discussion

4.1 Malformations in *H. carteri* in response to CO_2 increase

In the recent years, several studies have focused on coccolithophores' responses under increasing CO_2 levels, demonstrating that different species, and often different strains of the same species, exhibit a specific at times contrasting response to seawater carbonate chemistry (e.g., Bach et al., 2015; Diner et al., 2015; Langer et al., 2006, 2009, 2011; Langer and Bode 2011; Müller et al., 2015). These non-uniform results have highlighted the need to analyze the CO_2 influence on both coccolithophore species and strains to better predict the whole group reaction to future climate change.

To evaluate the coccolithophore response under high CO_2, a key but sometimes neglected parameters are the degree of coccolith malformation and data on morphometrics. To date, few studies have evaluated coccolith morphology (i.e., normal, malformed, or incomplete coccoliths) under seawater carbonate chemistry changes not only in a qualitative way, but also in a quantitative way (e.g., Bach et al., 2011, 2012; De Bodt et al., 2010; Diner et al., 2015; Kottmeier et al., 2022; Langer et al., 2006, 2011), but none of them considered the species *H. carteri*. Coccolith morphology is central to ecological and evolutionary success of coccolithophores and is often more telling than calcite production when questions concern the

biology, as opposed to the biogeochemistry, of these algae (Henriksen et al., 2003; Langer et al., 2011, 2021; Walker et al., 2018).

In this work, for the first time, we show that the percentage of malformed coccoliths in *H. carteri* does not change in a significant way moving from 295 to 600 µatm CO_2. ~~In this work, for the first time, we show that the percentage of malformed coccoliths in *H. carteri* increases from 295 to 600 µatm of CO_2.~~ However, when comparing our findings for *H. carteri* with previous works conducted on other species, it is evident that for most species and strains the percentage of malformed coccoliths at CO_2 levels similar to 295 µatm (±100 µatm) is higher (Fig. 4a, b). Specifically, a greater percentage of malformed coccoliths (considering all the categories defined by the authors) was observed in six different strains of *E. huxleyi* (RCC1238, RCC1216, RCC 1256, RCC1212, B92/11, AC481), four strains of *C. leptoporus* (AC365, RCC1135, RCC1141, RCC1168), and one strain (AC400) of *C. pelagicus* (Fig. 4 a, b).

Here we will briefly discuss an issue that distinguishes C-system experiments from other standard culture experiments, namely the fact that the C-system is not one single parameter but multiple (see Table 1), as opposed to experiments studying the effects of temperature for instance. Different methods for changing the C-system are available, i.e. DIC manipulation, TA manipulation, and combined TA-DIC manipulation (Hoppe et al., 2011; Langer and Bode, 2011). Only the latter method allows for an identification of the parameter of the C-system affecting organisms (Langer and Bode, 2011). Very few studies have used this method, and it was found that CO_2 and pH are parameters of the C-system that affect coccolithophores in typical OA studies (Bach et al., 2011; Langer and Bode, 2011). Here we used DIC manipulation resulting in a so-called coupled C-system, as opposed to the decoupled C-system obtainable only in combined TA-DIC manipulation experiments. A coupled C-system features correlations between pH, CO_2, and CO_3^{2-}. It is therefore not possible to distinguish e.g. pH and CO_2 effects. Please note that when we discuss "CO_2 effects" we do not literally mean CO_2 effects but coupled C-system effects. We have decided to use the shorthand "CO_2 effects" because it is common in the literature to do so. Using the strictly correct expression C-system effects has the disadvantage of decreasing readability substantially because a typical phrasing such as "C-system increase/decrease" does not make sense, whereas it does make sense if a single parameter is used as a stand-in for the whole C-system.

When considering responses to CO_2 levels close to 600 µatm, the percentages of malformed coccoliths in *E. huxleyi* (RCC1238 and RCC1256) are lower than *H. carteri* (Fig. 4a, c). In contrast, *E. huxleyi* (B92/11) and the heavily calcified species *C. leptoporus* (RCC1168) and *C. quadriperforatus* (RCC1141) consistently show a higher percentage of malformed coccoliths compared to *H. carteri* (~60-90%, Fig. 4a, c). Today *C. leptoporus* and *C. quadriperforatus* are mostly considered separate species (https://roscoff-culture-collection.org/rcc-strain-details/1141), although some authors prefer to consider *quadriperforatus* a sub-species (https://www.mikrotax.org/; Young et al., 2022). For a detailed discussion of the taxonomical status of *Calcidiscus* see Geisen et al. (2004).

The comparison of malformations in different strains/species at one single CO_2 level is instructive but not sufficient to assess C-system effects. Malformations in coccolithophores vary both between strains/species and over time in a single strain under constant environmental conditions (Langer et al., 2009; 2013; Langer and Benner, 2009). A better assessment of C-system

effects on coccolithophores is achieved when comparing trends of different experiments rather than absolute values of different experiments (Hoppe et al., 2011). Such a comparison clearly suggests species specific responses to CO_2, identifying more/less sensitive species ~~When considering responses to CO_2 levels close to 600 µatm, the percentages of malformed coccoliths in *E. huxleyi* (RCC1238 and RCC1256) are lower than *H. carteri* (Fig. 4a, c). In contrast, the heavily calcified species *C. leptoporus* (RCC1168) and *C. quadriperforatus* (RCC1141) consistently show a higher percentage of malformed coccoliths compared to *H. carteri* (~ 90%, Fig. 4a, c). It is interesting to note that these percentages also include a significant amount of extremely malformed coccoliths (89% for *C. quadriperforatus* RCC1141, and 46% for *C. leptoporus* RCC1168; Fig. 4a). This degree of malformation has never been observed in our experiments. Since biological parameters such as coccolith morphology undergo numerical changes over time (Langer et al., 2013), the assessment of species sensitivity should not be based on the morphology of different strains or species at one CO_2 level alone, but rather the change of morphology in response to a change in CO_2 (Hoppe et al., 2011). For example, the species *E. huxleyi* strain B92/11 shows varying percentages of malformations across a narrow range of CO_2 levels, illustrating this observation (Fig. 4a, b). On the other hand, at ca. 600 µatm CO_2 *Calcidiscus* displays more malformations than at 295 µatm of CO_2 (Fig. 4c), and the reason for this is most likely that the negative effect of carbonate chemistry is almost invisible at ca. 300 µatm CO_2. Using the reasoning of Bach et al. (2015), we would say that at 300 µatm of CO_2 neither substrate limitation nor proton inhibition play a significant role, and the malformations depend on other experimental conditions.~~

~~On the contrary, at ca. 600 µatm CO_2 the effect of proton inhibition becomes visible in *Calcidiscus* compared to *Emiliania* and *Helicosphaera*. Therefore, the conclusion suggested by the morphology distribution in Fig. 4 is confirmed when comparing relative changes between experiments~~ (Fig. 4b, c; Diner et al., 2015; Hoppe et al., 2011; Langer et al., 2006, 2011; Langer and Bode, 2011). We are thus confident in saying that the strains RCC1238 and RCC1256 of *E. huxleyi* and RCC1323 of *H. carteri* are less sensitive to acidification than *E. huxleyi* B92/11 and *Calcidiscus.*

However, it is important to note that different authors have observed varying responses among different strains of both *E. huxleyi* and *C. leptoporus*, indicating the absence of a uniform species-specific behavior, potentially linked to genotypic diversity (see Diner et al., 2015; Langer et al., 2009). These diverse responses could be identified in *H. carteri* too. Therefore, additional studies considering different strains of *H. carteri* will be required to identify if our evidence is strain-specific or it can be extended to species level.

360

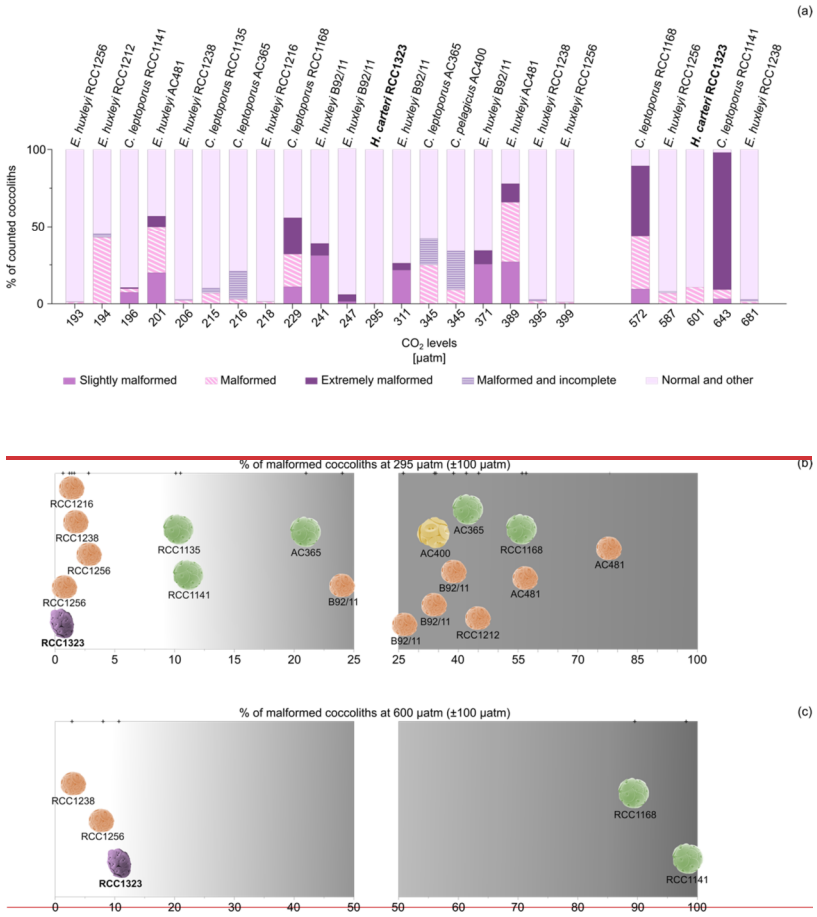

Formatted: Left, Line spacing: single

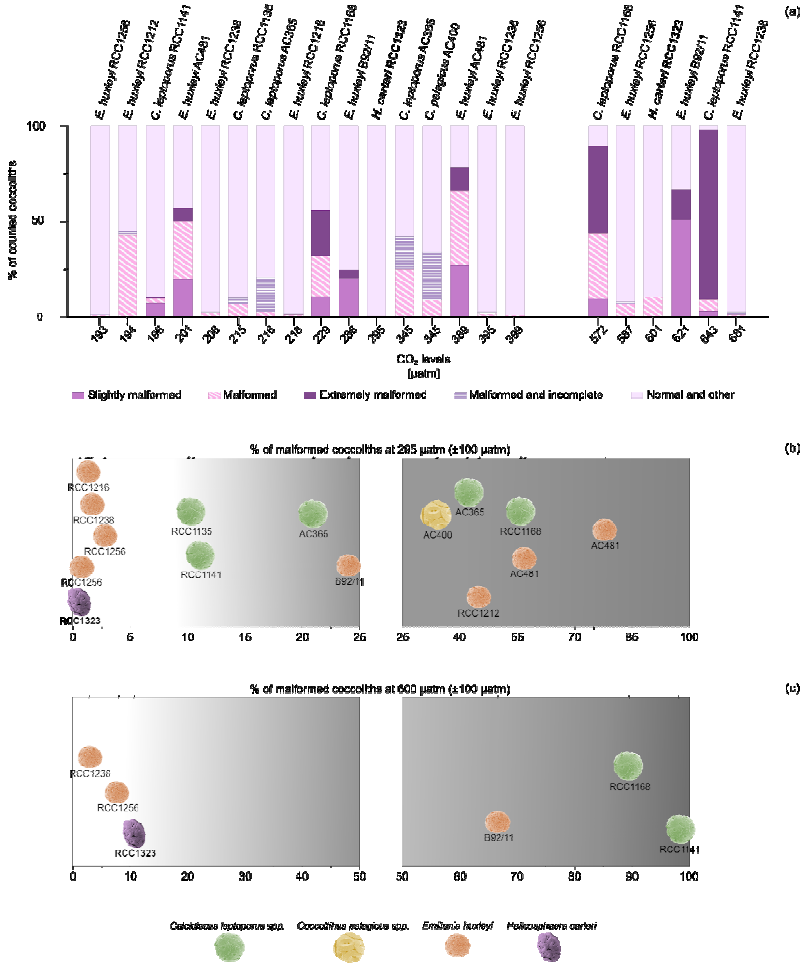

Figure 4. a) Percentages of malformed coccoliths in *H. carteri* (in bold; this work) compared to other species (from literature) at CO_2 levels close to 295 µatm (±100 µatm) and 600 µatm (±100 µatm). "Other" includes other categories used by the authors, such as fragmented coccoliths or incomplete coccoliths without malformations. b-c) Distribution of the considered strains according to a gradient of increasing percentage of malformation at 295 µatm (b) and 600 µatm (c). Different scales have been used. Coccosphere photos are modified from Nannotax.org. Data for comparison include *E. huxleyi* RCC1216, RCC1238, RCC1256 and RCC1212 from Langer et al. (2011); *C. leptoporus* RCC1141 and *C. quadriperforatus* RCC1168 from Diner et al. (2015); *E. huxleyi* AC481 from De Bodt et al. (2010); *C. leptoporus* RCC1135 from Langer and Bode (2011); *C. leptoporus* AC365 and *C. pelagicus* AC400 from Langer et al. (2006); *E. huxleyi* B92/11 from Bach et al. (2011).

4.2 *Helicosphaera carteri* sensitivity towards CO_2 increase

Studies on coccosphere and protoplast geometry (e.g., ~~ΘØ~~, C_L, C_N) of *H. carteri* strain RCC1323 have been conducted before (Le Guevel et al., 2024; Sheward et al., 2017; Šupraha et al., 2015). However, none of these studies considered the variations in protoplast or coccosphere shapes. In this study, we show for the first time the absence of any significant variation in $RD_{protoplast}$ and $RD_{coccosphere}$ with increasing CO_2 (Fig. 3a, b). These results could indicate that the species shape does not depend on CO_2 concentrations. Daily observation of the living culture under a light microscope showed in both CO_2 treatments a good health of *H. carteri*, including good motility of the cells. These observations combined with the lack of a CO_2 effect on roundness and the small effect on coccolith morphology point to a weak sensitivity of *H. carteri* to seawater acidification/CO_2 increase (Figs. 2, 3 a, b).

In our study, we also examined the variations in the protoplast and coccosphere geometry (C_N, C_L, coccosphere and protoplast size) in response to an increase in CO_2, observing no significant changes from 295 to 600 µatm (Fig. 3, Appendix A Table A1). Since *H. carteri* Θ, C_L and C_N did not change between our experiments, the cellular POC and PIC content and PIC:POC ratio did not show any substantial variation with increasing CO_2 (Fig. 3c, d; Table 3, Appendix A Table A1).

A non-significant variation in ~~coccosphere size and~~ PIC:POC ratio in the same *H. carteri* strain and at similar CO_2 levels (300 µatm and 600 µatm) has recently been observed also by Le Guevel et al. (2024) (Fig. 5). These authors grew the species to under even higher CO_2 levels, recording a decrease in coccosphere size (-1.05 µm) moving from 600 µatm to 1400 µatm of CO_2. However, this decrease in coccosphere size with increasing CO_2/decreasing pH, was not associated with a significant trend in the PIC:POC ratio (Le Guevel et al., 2024).

Similar results were documented also in the fossil record by Šupraha & Henderiks (2020), who estimated the PIC:POC ratio for the genus *Helicosphaera* over the last 15 million years (Myr) from the lateral cross-sectional aspect ratio of a coccolith (AR_L), following McClelland et al. (2016). These authors documented a stable PIC:POC ratio of this genus along with a reduction of coccolith (and coccosphere) size in response to the global decreasing trend in CO_2 (Herbert et al., 2016; Sosdian et al., 2018; Super et al., 2018; Zachos et al., 2001; Zhang et al., 2013). Šupraha & Henderiks (2020) attributed the lack of change in the ratio between calcification and photosynthesis to the obligate calcifier nature of the genus *Helicosphaera*.

Some coccolithophores such as *Coccolithus braarudii* are obligate calcifiers, i.e., they need to calcify, whereas others such as *Emiliania huxleyi* are facultative calcifiers, i.e., they do not necessarily need to calcify (Walker et al., 2018). As per our own observation, and the extensive observational record available at the RCC Roscoff (https://roscoff-culture-collection.org/; I. Probert, personal communication) *H. carteri* is an obligate calcifier which might imply a stable PIC/POC ratio because a complete coccosphere is essential for survival (Šupraha & Henderiks, 2020; Walker et al., 2018).

The obligate calcifier-nature of *Helicosphaera* represented by the maintenance of a stable PIC:POC observed both under experimental conditions; (this work, Le Guevel et al., 2024) and in the fossil record; (Šupraha & Henderiks, 2020), could represent an advantage in future oceans where the species could play a stable role in the C cycle despite changes in CO_2

concentrations. However, to confirm this hypothesis, studies on fossil material deposited during paleo-analogues of future CO_2 rise above 600 µatm are required. Reconstructing different coccolithophore species' PIC:POC ratio during past climate events is, indeed, a fundamental tool to better predict their response also to future climate changes. Unfortunately, the chances to find entirely preserved coccospheres in the fossil record is relatively low (Henderiks et al., 2008). Thus, combining culture studies on PIC:POC estimates from coccosphere, protoplast, AR, and coccolith measurements with observations conducted on fossil coccoliths represents a key tool for investigating the species-specific contribution to the organic C fixation and calcite production in the fossil record, improving our knowledge on the inorganic *versus* organic C balance in the oceans.

With regard to the relationships between PIC:POC ratio and CO_2 sensitivity of different species and strains one of the most significant and consistent evidence is that coccolithophore species with a higher PIC:POC ratio such as *C. leptoporus* (2.08) and *G. oceanica* (1.25) should be more sensitive to increasing CO_2 compared to species with lower average PIC:POC ratio such as *E. huxleyi* (0.67), *Syracosphaera pulchra* (0.19), and *Umbilicosphaera sibogae* (0.62; Gafar et al., 2019b). The latter authors hypothesize that a high PIC/POC ratio produces a high cellular proton load that is particularly harmful under Ocean Acidification conditions. More recently a cellular mechanism underpinning the hypothesis of Gafar et al. (2019b) was proposed (Kottmeier et al., 2022). This cellular mechanism involves Hv-type plasma-membrane proton channels which close under Ocean Acidification conditions therewith preventing proton export out of the cell with cytosolic acidification ensuing. The low sensitivity of species with lower PIC:POC ratio, like *E. huxleyi*, is confirmed by the comparison in Figure 4b, c, where *E. huxleyi* appears more resilient in terms of malformations to increasing CO_2 levels, compared to both *H. carteri* and *C. leptoporus*. As for *H. carteri* RCC1323, the range of PIC:POC ratio considered by Gafar et al. (2019b), based on data from Šupraha et al. (2015), spans from 2.29 to 2.30, thus a relatively high ratio leading to a first inference that this strain may be highly sensitive to CO_2 increase. However, recent data about *H. carteri* PIC:POC ratio documented a lower PIC:POC values for this strain (1.27-1.37 ratio this work; ~1.4-1.6 ratio Le Guevel et al., 2024) (Fig. 5). The identification of a lower PIC:POC ratio for *H. carteri* RCC1323 (average ratio 1.8) could explain our data documenting a low sensitivity of this strain to increasing CO_2, compared to *C. leptoporus* (average ratio 2.08) and *C. quadriperforatus* (average ratio 2.01) (see Sect. 4.1; Diner et al., 2015; Gafar et al., 2019b).

However, in the literature there are sometimes contrasting results on coccolithophore sensitivity towards CO_2 in relation to the PIC:POC ratio. Langer et al. (2009), while testing different strains of *E. huxleyi* grown under varying seawater chemistry conditions, documented that the strain with the highest PIC:POC ratio (RCC1216; maximum PIC:POC value 1.2) exhibited the highest percentage of normal coccoliths, corresponding to a low sensitivity towards higher CO_2. The most likely explanation for these observations is that other aspects than the PIC:POC ratio influence the species' response to increased CO_2 levels. For instance, genetic factors, as suggested by Diner et al. (2015) and Langer et al. (2009), may play a significant role. This once again underscores the importance of analyzing different species and strains and under varying experimental conditions.

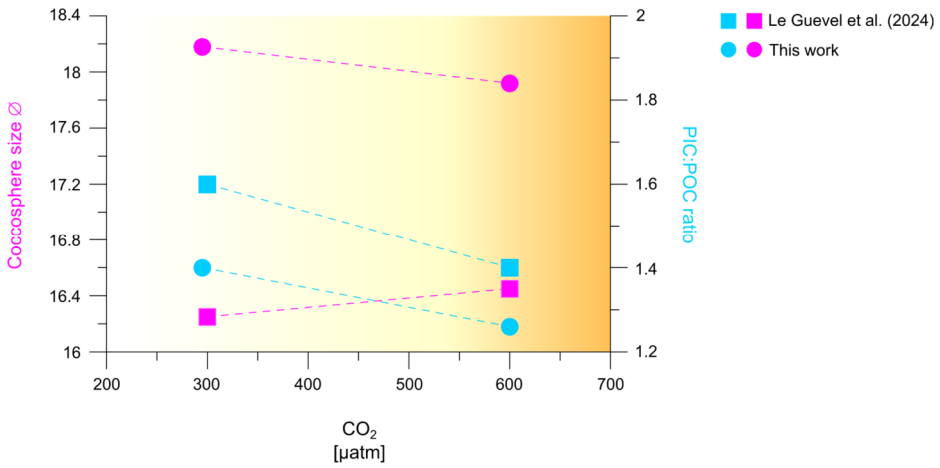

Figure 5. Comparison of coccosphere size and PIC:POC ratio of *H. carteri* under increasing CO_2, measured in this work and in Le Guevel et al. (2024).

5. Conclusions

Based on our findings, we can conclude that:

1. *Helicosphaera carteri*, exposed to pre-industrial CO_2 levels and 600µatm of CO_2, shows a low sensitivity to rising CO_2, as inferred from protoplast and coccosphere roundness, and chiefly from coccolith morphology.
2. The low sensitivity of *H. carteri* to high CO_2 is contrasted with the relatively high sensitivity of *Calcidiscus*. An explanation for this surprising species specificity might be the low PIC:POC of *H. carteri* determined here.
3. The PIC:POC ratio of *H. carteri* does not change with changing CO_2 suggesting a constant contribution of this species to the rain ratio under ocean acidification.

Appendix A: morphometric analyses

CO_2 [µatm]		**295**	**600**
Coccosphere size Ø [µm]	Min	14.30	14.76
	Mean	18.18	17.92
	Max	21.54	23.30
	SD	0.25	0.66

CO_2 [µatm]		**295**	**600**
Protoplast size Θ [µm]	Nr. of values	151	158
	Min	9.59	9.74
	Mean	11.45	11.81
	Max	14.12	14.56
	SD	0.19	0.27
Coccosphere aspect ratio $AR_{coccosphere}$	Nr. of values	161	154
	Min	1.01	1.01
	Mean	1.13	1.14
	Max	1.46	1.3
	SD	0.02	0.005
Coccosphere roundness $RD_{coccosphere}$	Nr. of values	151	158
	Min	0.69	0.74
	Mean	0.89	0.88
	Max	0.99	0.99
	SD	0.02	0.003
Protoplast aspect ratio $AR_{protoplastl}$	Nr. of values	151	158
	Min	1.00	1.01
	Mean	1.12	1.11
	Max	1.34	1.47
	SD	0.03	0.02
Protoplast roundness $RD_{protoplast}$	Nr. of values	161	154
	Min	0.75	0.68
	Mean	0.90	0.90
	Max	0.99	0.99
	SD	0.02	0.01
Coccoliths per coccosphere C_N	Nr. of values	161	154
	Min	9	9
	Mean	15	15
	Max	20	25
	SD	0.67	0.44

CO_2 [µatm]		295	600
Coccolith length C_L [µm]	Nr. of values	167	178
	Min	6.20	6.6
	Mean	8.65	8.60
	Max	10.01	10.33
	SD	0.07	0.04
Cellular PIC [pg cell^{-1}]	Nr. of values	201	207
	Mean	151.86	149.47
	SD	4.23	9.50
Cellular POC [pg cell^{-1}]	Nr. of values	201	207
	Mean	108.14	118.51
	SD	5.42	6.41
	Nr. of values	161	154

Table A1. Summary of *H. carteri* protoplast and coccosphere geometry data obtained from ImageJ Software used in this work. The values reported are the averages of the replicates. SD= standard deviation.

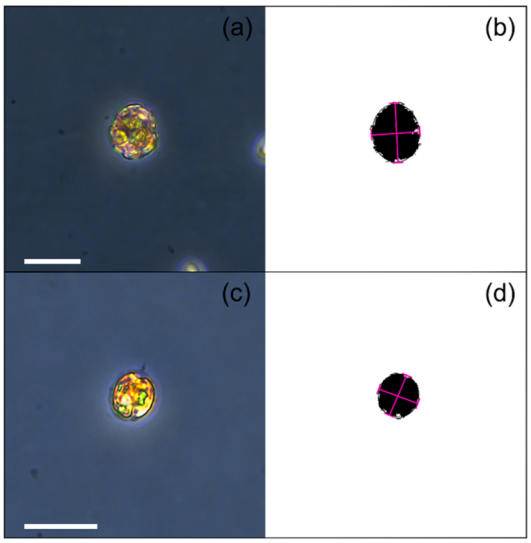

4.

Figure A1. Photo of a coccosphere (a, b) and a protoplast (c, d) before and after ImageJ processing. Measurements of the long and short axes are indicated in pink (c, d). All bars are 20 µm.

Data availability

The Java script used here within ImageJ Software is available on GitHub: https://github.com/mbordiga/Coccoliths

Author contribution

S.B., G.L. and M.B. conceived the study; F.C. and M.B. designed the experiments and M.B. carried out the experiments; S.B. and G.L. analyzed the coccolithophore samples, the data sets, and elaborated the data; S.B. wrote the first draft with contributions on data discussion and interpretation from G.L., M.B., and C.L.; M.B., C.L., and A.D.G. provided financial support for the project; P.Z. and A.D.G. provided a critical review. All authors contributed to the final draft.

Competing interests

The authors declare that they have no conflict of interest.

Disclaimer

Publisher's note: Copernicus Publications remains neutral with regard to jurisdictional claims made in the text, published maps, institutional affiliations, or any other geographical representation in this paper. While Copernicus Publications makes every effort to include appropriate place names, the final responsibility
lies with the authors.

Acknowledgments

We thank M. P. Riccardi and M. Musa (CISRiC-Arvedi Laboratory, University of Pavia) for technical assistance during SEM analyses; M. Cabrini, A. Beran, F. Relitti, and V. A. Laudicella (OGS, Trieste) for their technical support. This work was funded by MUR for ECORD-IODP Italia 2018 to M. Bordiga within the project "Geochemistry and marine biology united to refine climate models" conducted at the National Institute of Oceanography and Applied Geophysics (OGS) and for Italian national inter-university PhD course in Sustainable Development and Climate change (link: www.phd-sdc.it) to S. Bianco. The project was also supported by C. Lupi and A. Di Giulio with University of Pavia Research Funds (FAR 2021-2023) and by the Okada-McIntyre Graduate Research Fellowship of INA awarded to S. Bianco. G. Langer acknowledges funding from the Spanish Ministry of Universities through a Maria Zambrano grant and the Generalitat de Catalunya (MERS, 2021 SGR 00640). This work contributes to ICTA-UAB "María de Maeztu" Programme for Units of Excellence of the Spanish Ministry of Science and Innovation (CEX2019-000940-M).

This paper and related research have been conducted during and with the support of the Italian national inter-university PhD course in Sustainable Development and Climate change (link: www.phd-sdc.it), and it is part of S. Bianco PhD.

References

Andruleit, H. and Rogalla, U.: Coccolithophores in surface sediments of the Arabian Sea in relation to environmental gradients in surface waters, Marine Geology, 186, 505–526, https://doi.org/10.1016/S0025-3227(02)00312-2, 2002.

Aubry, M.-P.: Phylogeny of the Cenozoic calcareous nannoplankton genus *Helicosphaera*, Paleobiology, 14, 64–80, https://doi.org/10.1017/S0094837300011805, 1988.

Bach, L. T., Riebesell, U., and Schulz, K. G.: Distinguishing between the effects of ocean acidification and ocean carbonation in the coccolithophore *Emiliania huxleyi*, Limnology & Oceanography, 56, 2040–2050, https://doi.org/10.4319/lo.2011.56.6.2040, 2011.

Bach, L. T., Bauke, C., Meier, K. J. S., Riebesell, U., and Schulz, K. G.: Influence of changing carbonate chemistry on morphology and weight of coccoliths formed by *Emiliania huxleyi*, Biogeosciences, 9, 3449–3463, https://doi.org/10.5194/bg-9-3449-2012, 2012.

Bach, L. T., Riebesell, U., Gutowska, M. A., Federwisch, L., and Schulz, K. G.: A unifying concept of coccolithophore sensitivity to changing carbonate chemistry embedded in an ecological framework, Progress in Oceanography, 135, 125–138, https://doi.org/10.1016/j.pocean.2015.04.012, 2015.

Baumann, K.-H., Böckel, B., and Frenz, M.: Coccolith contribution to South Atlantic carbonate sedimentation, in: Coccolithophores, edited by: Thierstein, H. R. and Young, J. R., Springer Berlin Heidelberg, Berlin, Heidelberg, 367–402, https://doi.org/10.1007/978-3-662-06278-4_14, 2004.

Baumann, K.-H., Andruleit, H., Böckel, B., Geisen, M., and Kinkel, H.: The significance of extant coccolithophores as indicators of ocean water masses, surface water temperature, and palaeoproductivity: a review, Paläontol. Z., 79, 93–112, https://doi.org/10.1007/BF03021756, 2005.

Bown, P. R., Lees, J. A., and Young, J. R.: Calcareous nannoplankton evolution and diversity through time, in: Coccolithophores, edited by: Thierstein, H. R. and Young, J. R., Springer Berlin Heidelberg, Berlin, Heidelberg, 481–508, https://doi.org/10.1007/978-3-662-06278-4_18, 2004.

Brand, L. E.: Physiological ecology of marine coccolithophores, in: Coccolithophores, edited by: Winter, A. and Siesser, W. G., pp. 39–50, Cambridge University Press, Cambridge, 1994.

Buitenhuis, E. T., De Baar, H. J. W., and Veldhuis, M. J. W.: Photosynthesis and calcification by *Emiliania huxleyi* (Prymnesiophyceae) as a function of inorganic carbon species, J. Phycol., 35, 949–959, https://doi.org/10.1046/j.1529-8817.1999.3550949.x, 1999.

Canadell, J. G., Le Quéré, C., Raupach, M. R., Field, C. B., Buitenhuis, E. T., Ciais, P., Conway, T. J., Gillett, N. P., Houghton, R. A., and Marland, G.: Contributions to accelerating atmospheric CO_2 growth from economic activity, carbon

intensity, and efficiency of natural sinks, Proc. Natl. Acad. Sci. U.S.A., 104, 18866–18870, https://doi.org/10.1073/pnas.0702737104, 2007.

CoSMi Trieste: https://cosmi.ogs.it/it, 2024.

D'Amario, B., Pérez, C., Grelaud, M., Pitta, P., Krasakopoulou, E., and Ziveri, P.: Coccolithophore community response to ocean acidification and warming in the Eastern Mediterranean Sea: results from a mesocosm experiment, Sci Rep, 10, 12637, https://doi.org/10.1038/s41598-020-69519-5, 2020.

Daniels, C., Poulton, A., Young, J., Esposito, M., Humphreys, M., Ribas-Ribas, M., Tynan, E., and Tyrrell, T.: Species-specific calcite production reveals *Coccolithus pelagicus* as the key calcifier in the Arctic Ocean, Mar. Ecol. Prog. Ser., 555, 29–47, https://doi.org/10.3354/meps11820, 2016.

Daniels, C. J., Sheward, R. M., and Poulton, A. J.: Biogeochemical implications of comparative growth rates of *Emiliania huxleyi* and *Coccolithus* species, Biogeosciences, 11, 6915–6925, https://doi.org/10.5194/bg-11-6915-2014, 2014.

De Bodt, C., Van Oostende, N., Harlay, J., Sabbe, K., and Chou, L.: Individual and interacting effects of CO_2 and temperature on *Emiliania huxleyi* calcification: study of the calcite production, the coccolith morphology and the coccosphere size, Biogeosciences, 7, 1401–1412, https://doi.org/10.5194/bg-7-1401-2010, 2010.

De Vries, J., Poulton, A. J., Young, J. R., Monteiro, F. M., Sheward, R. M., Johnson, R., Hagino, K., Ziveri, P., and Wolf, L. J.: CASCADE: Dataset of extant coccolithophore size, carbon content and global distribution, Sci Data, 11, 920, https://doi.org/10.1038/s41597-024-03724-z, 2024.

Dickson, A. G., Sabine, C. L., & Christian, J. R.: Guide to best practices for ocean CO_2 measurement., North Pacific Marine Science Organization, https://doi.org/10.25607/OBP-1342, 2007.

Dickson, A. G. and Goyet, C.: Handbook of methods for the analysis of the various parameters of the carbon dioxide system in sea water. Version 2, https://doi.org/10.2172/10107773, 1994.

Dickson, A. G. and Millero, F. J.: A comparison of the equilibrium constants for the dissociation of carbonic acid in seawater media, Deep Sea Research Part A. Oceanographic Research Papers, 34, 1733–1743, https://doi.org/10.1016/0198-0149(87)90021-5, 1987.

Dimiza, M. D., Triantaphyllou, M. V., & Malinverno, E.: New evidence for the ecology of *Helicosphaera carteri* in polluted coastal environments (Elefsis Bay, Saronikos Gulf, Greece). Journal of Nannoplankton Research, 34, 37-43, 2014.

Diner, R. E., Benner, I., Passow, U., Komada, T., Carpenter, E. J., and Stillman, J. H.: Negative effects of ocean acidification on calcification vary within the coccolithophore genus *Calcidiscus*, Mar Biol, 162, 1287–1305, https://doi.org/10.1007/s00227-015-2669-x, 2015.

Dong, S., Lei, Y., Li, T., Cao, Y., and Xu, K.: Biocalcification crisis in the continental shelf under ocean acidification, Geoscience Frontiers, 14, 101622, https://doi.org/10.1016/j.gsf.2023.101622, 2023.

Findlay, C. S. and Giraudeau, J.: Extant calcareous nannoplankton in the Australian Sector of the Southern Ocean (austral summers 1994 and 1995), Marine Micropaleontology, 40, 417–439, https://doi.org/10.1016/S0377-8398(00)00046-3, 2000.

Field Code Changed

Findlay, C. S. and Giraudeau, J.: Movement of oceanic fronts south of Australia during the last 10 ka: interpretation of calcareous nannoplankton in surface sediments from the Southern Ocean, Marine Micropaleontology, 46, 431–444, https://doi.org/10.1016/S0377-8398(02)00084-1, 2002.

Fiorini, S., Middelburg, J. J., and Gattuso, J.: testing the effects of elevated pCO_2 on coccolithophores (prymnesiophyceae): comparison between haploid and diploid life stages, Journal of Phycology, 47, 1281–1291, https://doi.org/10.1111/j.1529-8817.2011.01080.x, 2011.

Gafar, N. A., Eyre, B. D., and Schulz, K. G.: A comparison of species specific sensitivities to changing light and carbonate chemistry in calcifying marine phytoplankton, Sci Rep, 9, 2486, https://doi.org/10.1038/s41598-019-38661-0, 2019a.

Gafar, N. A., Eyre, B. D., and Schulz, K. G.: Particulate inorganic to organic carbon production as a predictor for coccolithophorid sensitivity to ongoing ocean acidification, Limnol Oceanogr Letters, 4, 62–70, https://doi.org/10.1002/lol2.10105, 2019b.

García-Romero, F., Cortés, M. Y., Rochín-Bañaga, H., Bollmann, J., Aguirre-Bahena, F., Lara-Lara, R., and Herguera, J. C.: Vertical fluxes of coccolithophores and foraminifera and their contributions to $CaCO_3$ flux off the coast of Ensenada, Mexico, Cienc. Mar., 43, https://doi.org/10.7773/cm.v43i4.2765, 2017.

Gattuso, J.: Effect of calcium carbonate saturation of seawater on coral calcification, Global and Planetary Change, 18, 37–46, https://doi.org/10.1016/S0921-8181(98)00035-6, 1998.

Gazeau, F., Urrutti, P., Dousset, A., Brodu, N., Richard, M., Villeneuve, R., Pruvost, É., Comeau, S., Koechlin, H., and Pernet, F.: Toward an ecologically realistic experimental system to investigate the multigenerational effects of ocean warming and acidification on benthic invertebrates, Limnology & Ocean Methods, lom3.10630, https://doi.org/10.1002/lom3.10630, 2024.

Geisen, M., Young, J. R., Probert, I., Sáez, A. G., Baumann, K.-H., Sprengel, C., Bollmann, J., Cros, L., De Vargas, C., and Medlin, L. K.: Species level variation in coccolithophores, in: Coccolithophores, edited by: Thierstein, H. R. and Young, J. R., Springer Berlin Heidelberg, Berlin, Heidelberg, 327–366, https://doi.org/10.1007/978-3-662-06278-4_13, 2004.

Henderiks, J.: Coccolithophore size rules — Reconstructing ancient cell geometry and cellular calcite quota from fossil coccoliths, Marine Micropaleontology, 67, 143–154, https://doi.org/10.1016/j.marmicro.2008.01.005, 2008.

Henriksen, K., Stipp, S. L. S., Young, J. R., and Bown, P. R.: Tailoring calcite: Nanoscale AFM of coccolith biocrystals, American Mineralogist, 88, 2040–2044, https://doi.org/10.2138/am-2003-11-1248, 2003.

Herbert, T. D., Lawrence, K. T., Tzanova, A., Peterson, L. C., Caballero-Gill, R., and Kelly, C. S.: Late Miocene global cooling and the rise of modern ecosystems, Nature Geosci, 9, 843–847, https://doi.org/10.1038/ngeo2813, 2016.

Hoffmann, R., Kirchlechner, C., Langer, G., Wochnik, A. S., Griesshaber, E., Schmahl, W. W., and Scheu, C.: Insight into *Emiliania huxleyi* coccospheres by focused ion beam sectioning, Biogeosciences, 12, 825–834, https://doi.org/10.5194/bg-12-825-2015, 2015.

Hoppe, C. J. M., Langer, G., and Rost, B.: *Emiliania huxley*i shows identical responses to elevated pCO_2 in TA and DIC manipulations, Journal of Experimental Marine Biology and Ecology, 406, 54–62, https://doi.org/10.1016/j.jembe.2011.06.008, 2011.

Iglesias-Rodriguez, M. D., Halloran, P. R., Rickaby, R. E. M., Hall, I. R., Colmenero-Hidalgo, E., Gittins, J. R., Green, D. R. H., Tyrrell, T., Gibbs, S. J., Von Dassow, P., Rehm, E., Armbrust, E. V., and Boessenkool, K. P.: Phytoplankton Calcification in a High-CO_2 World, Science, 320, 336–340, https://doi.org/10.1126/science.1154122, 2008.

Intergovernmental Panel On Climate Change (Ipcc): Climate Change 2021 – The Physical Science Basis: Working Group I Contribution to the Sixth Assessment Report of the Intergovernmental Panel on Climate Change, 1st ed., Cambridge University Press, https://doi.org/10.1017/9781009157896, 2021.

Johnson, R., Langer, G., Rossi, S., Probert, I., Mammone, M., and Ziveri, P.: Nutritional response of a coccolithophore to changing PH and temperature, Limnology & Oceanography, 67, 2309–2324, https://doi.org/10.1002/lno.12204, 2022.

Jokiel, P. L., Rodgers, K. S., Kuffner, I. B., Andersson, A. J., Cox, E. F., and Mackenzie, F. T.: Ocean acidification and calcifying reef organisms: a mesocosm investigation, Coral Reefs, 27, 473–483, https://doi.org/10.1007/s00338-008-0380-9, 2008.

Keul, N., Langer, G., De Nooijer, L. J., and Bijma, J.: Effect of ocean acidification on the benthic foraminifera *Ammonia* sp. is caused by a decrease in carbonate ion concentration, Biogeosciences, 10, 6185–6198, https://doi.org/10.5194/bg-10-6185-2013, 2013.

Kottmeier, D. M., Chrachri, A., Langer, G., Helliwell, K. E., Wheeler, G. L., and Brownlee, C.: Reduced H^+ channel activity disrupts pH homeostasis and calcification in coccolithophores at low ocean pH, Proc. Natl. Acad. Sci. U.S.A., 119, e2118009119, https://doi.org/10.1073/pnas.2118009119, 2022.

Kroeker, K. J., Kordas, R. L., Crim, R., Hendriks, I. E., Ramajo, L., Singh, G. S., Duarte, C. M., and Gattuso, J.: Impacts of ocean acidification on marine organisms: quantifying sensitivities and interaction with warming, Global Change Biology, 19, 1884–1896, https://doi.org/10.1111/gcb.12179, 2013.

Krug, S. A., Schulz, K. G., and Riebesell, U.: Effects of changes in carbonate chemistry speciation on *Coccolithus braarudii*: a discussion of coccolithophorid sensitivities, Biogeosciences, 8, 771–777, https://doi.org/10.5194/bg-8-771-2011, 2011.

Langdon, C., Takahashi, T., Sweeney, C., Chipman, D., Goddard, J., Marubini, F., Aceves, H., Barnett, H., and Atkinson, M. J.: Effect of calcium carbonate saturation state on the calcification rate of an experimental coral reef, Global Biogeochemical Cycles, 14, 639–654, https://doi.org/10.1029/1999GB001195, 2000.

Langer, G. and Benner, I.: Effect of elevated nitrate concentration on calcification in *Emiliania huxleyi* ., J. Nannoplankton Res., 30, 77–82, https://doi.org/10.58998/jnr2158, 2009.

Langer, G. and Bode, M.: CO_2 mediation of adverse effects of seawater acidification in *Calcidiscus leptoporus*, Geochem Geophys Geosyst, 12, 2010GC003393, https://doi.org/10.1029/2010GC003393, 2011.

Formatted: Font: Italic

Langer, G., Geisen, M., Baumann, K., Kläs, J., Riebesell, U., Thoms, S., and Young, J. R.: Species-specific responses of calcifying algae to changing seawater carbonate chemistry, Geochem Geophys Geosyst, 7, 2005GC001227, https://doi.org/10.1029/2005GC001227, 2006.

Langer, G., Nehrke, G., Probert, I., Ly, J., and Ziveri, P.: Strain-specific responses of *Emiliania huxleyi* to changing seawater carbonate chemistry, Biogeosciences, 6, 2637–2646, https://doi.org/10.5194/bg-6-2637-2009, 2009.

Langer, G., Probert, I., Nehrke, G., and Ziveri, P.: The morphological response of *Emiliania huxleyi* to seawater carbonate chemistry changes: an inter-strain comparison., J. Nannoplankton Res., 32, 29–36, https://doi.org/10.58998/jnr2159, 2011.

Langer, G., Oetjen, K., and Brenneis, T.: On culture artefacts in coccolith morphology, Helgol Mar Res, 67, 359–369, https://doi.org/10.1007/s10152-012-0328-x, 2013.

Langer, G., Taylor, A. R., Walker, C. E., Meyer, E. M., Ben Joseph, O., Gal, A., Harper, G. M., Probert, I., Brownlee, C., and Wheeler, G. L.: Role of silicon in the development of complex crystal shapes in coccolithophores, New Phytologist, 231, 1845–1857, https://doi.org/10.1111/nph.17230, 2021.

Le Guevel, G., Minoletti, F., Geisen, C., Duong, G., Rojas, V., and Hermoso, M.: Multispecies expression of coccolithophore vital effects with changing CO_2 concentrations and pH in the laboratory with insights for reconstructing CO_2 levels in geological history, https://doi.org/10.5194/egusphere-2024-1890, 28 June 2024.

Lewis, E. R. and Wallace, D. W. R.: Program Developed for CO_2 System Calculations, https://doi.org/10.15485/1464255, 1998.

McClelland, H. L. O., Barbarin, N., Beaufort, L., Hermoso, M., Ferretti, P., Greaves, M., and Rickaby, R. E. M.: Calcification response of a key phytoplankton family to millennial-scale environmental change, Sci Rep, 6, 34263, https://doi.org/10.1038/srep34263, 2016.

Mehrbach, C., Culberson, C. H., Hawley, J. E., and Pytkowicx, R. M.: Measurement of the apparent dissociation constants of carbonic acid in seawater at atmospheric pressure 1, Limnology & Oceanography, 18, 897–907, https://doi.org/10.4319/lo.1973.18.6.0897, 1973.

Menden-Deuer, S. and Lessard, E. J.: Carbon to volume relationships for dinoflagellates, diatoms, and other protist plankton, Limnology & Oceanography, 45, 569–579, https://doi.org/10.4319/lo.2000.45.3.0569, 2000.

Menschel, E., González, H. E., and Giesecke, R.: Coastal-oceanic distribution gradient of coccolithophores and their role in the carbonate flux of the upwelling system off Concepción, Chile (36°S), J. Plankton Res., 38, 798–817, https://doi.org/10.1093/plankt/fbw037, 2016.

Meyer, J. and Riebesell, U.: Reviews and Syntheses: Responses of coccolithophores to ocean acidification: a meta-analysis, Biogeosciences, 12, 1671–1682, https://doi.org/10.5194/bg-12-1671-2015, 2015.

Mikrotax Project, "CASCADE Dataset Viewer for *Helicosphaera carteri*," available at: https://www.mikrotax.org/system/CASCADE/CASCdatasets.php?dataset_id=%25&taxon=helicosphaera+carteri&basemap=Gplatesbathymetry&scale=1, last access: 3 December 2024.

Milner, S., Langer, G., Grelaud, M., and Ziveri, P.: Ocean warming modulates the effects of acidification on *Emiliania huxleyi* calcification and sinking, Limnol. Oceanogr., 61, 1322–1336, https://doi.org/10.1002/lno.10292, 2016.

Monteiro, F. M., Bach, L. T., Brownlee, C., Bown, P., Rickaby, R. E. M., Poulton, A. J., Tyrrell, T., Beaufort, L., Dutkiewicz, S., Gibbs, S., Gutowska, M. A., Lee, R., Riebesell, U., Young, J., and Ridgwell, A.: Why marine phytoplankton calcify, Sci. Adv., 2, e1501822, https://doi.org/10.1126/sciadv.1501822, 2016.

Müller, M., Trull, T., and Hallegraeff, G.: Differing responses of three Southern Ocean *Emiliania huxleyi* ecotypes to changing seawater carbonate chemistry, Mar. Ecol. Prog. Ser., 531, 81–90, https://doi.org/10.3354/meps11309, 2015.

Nannotax3 website: www.mikrotax.org/Nannotax3, 2024.

Raven, J. and Crawfurd, K.: Environmental controls on coccolithophore calcification, Mar. Ecol. Prog. Ser., 470, 137–166, https://doi.org/10.3354/meps09993, 2012.

Riebesell, U., Zondervan, I., Rost, B., Tortell, P. D., Zeebe, R. E., and Morel, F. M. M.: Reduced calcification of marine plankton in response to increased atmospheric CO_2, Nature, 407, 364–367, https://doi.org/10.1038/35030078, 2000.

Ries, J. B.: A physicochemical framework for interpreting the biological calcification response to CO_2-induced ocean acidification, Geochimica et Cosmochimica Acta, 75, 4053–4064, https://doi.org/10.1016/j.gca.2011.04.025, 2011.

Rigual Hernández, A. S., Trull, T. W., Nodder, S. D., Flores, J. A., Bostock, H., Abrantes, F., Eriksen, R. S., Sierro, F. J., Davies, D. M., Ballegeer, A.-M., Fuertes, M. A., and Northcote, L. C.: Coccolithophore biodiversity controls carbonate export in the Southern Ocean, Biogeosciences, 17, 245–263, https://doi.org/10.5194/bg-17-245-2020, 2020.

Roscoff Culture Collection, available at: https://roscoff-culture-collection.org/rcc-strain-details/1141, last access: 5 December 2024.

Roscoff Culture Collection, available at: https://roscoff-culture-collection.org/, last access: 3 December 2024; I. Probert, personal communication.

Rueden, C. T., Schindelin, J., Hiner, M. C., DeZonia, B. E., Walter, A. E., Arena, E. T., and Eliceiri, K. W.: ImageJ2: ImageJ for the next generation of scientific image data, BMC Bioinformatics, 18, 529, https://doi.org/10.1186/s12859-017-1934-z, 2017.

Sabine, C. L., Feely, R. A., Gruber, N., Key, R. M., Lee, K., Bullister, J. L., Wanninkhof, R., Wong, C. S., Wallace, D. W. R., Tilbrook, B., Millero, F. J., Peng, T.-H., Kozyr, A., Ono, T., and Rios, A. F.: The Oceanic Sink for Anthropogenic CO_2, Science, 305, 367–371, https://doi.org/10.1126/science.1097403, 2004.

Sheward, R. M., Poulton, A. J., Gibbs, S. J., Daniels, C. J., and Bown, P. R.: Physiology regulates the relationship between coccosphere geometry and growth phase in coccolithophores, Biogeosciences, 14, 1493–1509, https://doi.org/10.5194/bg-14-1493-2017, 2017.

Sosdian, S. M., Greenop, R., Hain, M. P., Foster, G. L., Pearson, P. N., and Lear, C. H.: Constraining the evolution of Neogene Ocean carbonate chemistry using the boron isotope pH proxy, Earth and Planetary Science Letters, 498, 362–376, https://doi.org/10.1016/j.epsl.2018.06.017, 2018.

Sun, J. and Liu, D.: Geometric models for calculating cell biovolume and surface area for phytoplankton, J. Plankton Res., 25, 1331–1346, doi:10.1093/plankt/fbg096, 2003.

Super, J. R., Thomas, E., Pagani, M., Huber, M., O'Brien, C., and Hull, P. M.: North Atlantic temperature and pCO_2 coupling in the early-middle Miocene, Geology, 46, 519–522, https://doi.org/10.1130/G40228.1, 2018.

Šupraha, L. and Henderiks, J.: A 15-million-year-long record of phenotypic evolution in the heavily calcified coccolithophore *Helicosphaera* and its biogeochemical implications, Biogeosciences, 17, 2955–2969, https://doi.org/10.5194/bg-17-2955-2020, 2020.

Šupraha, L., Gerecht, A. C., Probert, I., and Henderiks, J.: Eco-physiological adaptation shapes the response of calcifying algae to nutrient limitation, Sci Rep, 5, 16499, https://doi.org/10.1038/srep16499, 2015.

Walker, C. E., Taylor, A. R., Langer, G., Durak, G. M., Heath, S., Probert, I., Tyrrell, T., Brownlee, C., and Wheeler, G. L.: The requirement for calcification differs between ecologically important coccolithophore species, New Phytologist, 220, 147–162, https://doi.org/10.1111/nph.15272, 2018.

Young, J.R. Functions of Coccoliths. In: Winter, A. and Siesser, W.G., Eds., Coccolithophores, Cambridge University Press, New York, 13-27, 1994.

Young, J. R.: Neogene, in: Calcareous Nannofossil Biostratigraphy, edited by: Bown, P. R., Springer Netherlands, Dordrecht, 225–265, https://doi.org/10.1007/978-94-011-4902-0_8, 1998.

Young, J. R. and Ziveri, P.: Calculation of coccolith volume and its use in calibration of carbonate flux estimates, 2000.

Zachos, J., Pagani, M., Sloan, L., Thomas, E., and Billups, K.: Trends, Rhythms, and Aberrations in Global Climate 65 Ma to Present, Science, 292, 686–693, https://doi.org/10.1126/science.1059412, 2001.

Zhang, Y. G., Pagani, M., Liu, Z., Bohaty, S. M., and DeConto, R.: A 40-million-year history of atmospheric CO_2, Phil. Trans. R. Soc. A., 371, 20130096, https://doi.org/10.1098/rsta.2013.0096, 2013.

Ziveri, P., Thunell, R. C., and Rio, D.: Export production of coccolithophores in an upwelling region: Results from San Pedro Basin, Southern California Borderlands, Marine Micropaleontology, 24, 335–358, https://doi.org/10.1016/0377-8398(94)00017-H, 1995.

Ziveri, P., Baumann, K.-H., Böckel, B., Bollmann, J., and Young, J. R.: Biogeography of selected Holocene coccoliths in the Atlantic Ocean, in: Coccolithophores, edited by: Thierstein, H. R. and Young, J. R., Springer Berlin Heidelberg, Berlin, Heidelberg, 403–428, https://doi.org/10.1007/978-3-662-06278-4_15, 2004.

Ziveri, P., De Bernardi, B., Baumann, K.-H., Stoll, H. M., and Mortyn, P. G.: Sinking of coccolith carbonate and potential contribution to organic carbon ballasting in the deep ocean, Deep Sea Research Part II: Topical Studies in Oceanography, 54, 659–675, https://doi.org/10.1016/j.dsr2.2007.01.006, 2007.

Zondervan, I., Rost, B., and Riebesell, U.: Effect of CO_2 concentration on the PIC/POC ratio in the coccolithophore *Emiliania huxleyi* grown under light-limiting conditions and different daylengths, J. Exp. Mar. Biol. Ecol., 272, 55–70, https://doi.org/10.1016/S0022-0981(02)00037-0, 2002.